Energy transfer in Ar-Cl^+ collisions

K. Balasubramanian and Pingyi Feng
Department of Chemistry, Arizona State University, Tempe, Arizona 85287-1604

Joyce J. Kaufman, P. C. Hariharan, and W. S. Koski
Department of Chemistry, The Johns Hopkins University, Baltimore, Maryland 21218

(Received 2 November 1987)

Experimentally, the transitions between ^3P and ^1D terms of Cl^+ have been observed in the inelastic collision between Cl^+ and Ar. The transfers are modeled through Landau-Zener types of processes at the points where the potential-energy surfaces of the electronic states of $ArCl^+$ cross. The potential-energy curves of ten electronic states of $ArCl^+$ arising from $Ar(^1S) + Cl^+(^3P)$, $Ar(^1S) + Cl^+(^1D)$, and $Ar^+(^2P) + Cl(^2P)$ dissociations are computed using the complete active-space multiconfiguration self-consistent field method followed by first-order configuration-interaction calculations. In addition, relativistic configuration-interaction calculations are carried out for the low-lying states of $ArCl^+$, with the objective of computing spin-orbit effects. These calculations reveal the existence of three bound states ($^3\Pi$, $^1\Sigma^+$, and $^1\Pi$) for which spectroscopic constants and dipole moments are obtained. The ground state is a $^3\Pi$ state with a dissociation energy of 0.32 eV, while the excited $^1\Sigma^+$ is bound at least by 1.81 eV with respect to $Ar(^1S) + Cl^+(^1D)$. The calculations predict that $ArCl^+$ is stable and long lived. The Mulliken population analysis of the electronic states of $ArCl^+$ reveals considerable charge transfer from Ar to Cl^+ in the $^1\Sigma^+$ and $^1\Pi$ states.

I. INTRODUCTION

The neutral rare-gas halide and oxide molecules have been the topics of many investigations in recent years.[1-7] The rare-gas oxide species have been investigated[6,7] as possible candidates for chemical lasers. The rare-gas atoms form, in many cases, stable long-lived ions in reactions with halogen positive ions. The results RX^+ ions are isoelectronic with halogen oxides and could thus be candidates for chemical lasers.

Since the discovery of stable XeF and KrF, mass-spectrometric studies have shown that XeF^+ and KrF^+ species are quite stable and long lived.[8] The noble gas ions $KrCl^+$, KrF^+, $ArCl^+$, and ArI^+ have also been reported to be stable.[9,10] Berkowitz, Chupka, and coworkers[11,12] have measured the binding energies of KrF^+, XeF^+, XeI^+, and ArF^+. The ArF^+ species has a binding energy of ≥ 1.66 eV while attempts to produce NeF^+ and HeF^+ have been unsuccessful. Watkins and Koski[13] have prepared the $KrBr^+$ ion and measured its binding energy.

We have observed that the collisions of X^+ with R atoms involve considerable transfer of translational to electronic energies and vice versa. The mechanisms of the energy transfer have not been well understood for all the species.

In earlier investigations, Balasubramanian *et al.*[13] and Hotokka *et al.*[14] have studied the Br^+-Kr collisions and F^+-Ne collisions, respectively. The potential-energy surfaces of these two species have been obtained. These studies have enabled interpretation of the energy transfers in these systems. The binding energy of the $^1\Sigma^+$ state of NeF^+ has been calculated to be 1.64 eV.[14]

The electronic states or potential-energy surfaces of $ArCl^+$ have not been investigated to date. There is very little information available on this ion. For example, what is the binding energy of the ion? What are the crossing points of the potential-energy surfaces of $ArCl^+$? The present theoretical investigation is undertaken with the intent of finding answers to these questions and comparing the results for $ArCl^+$ with those for NeF^+ and $KrBr^+$. The theoretical investigation of electronic states and potential-energy surfaces of molecules containing heavy atoms is a topic of considerable activity in recent years.[15-20]

We carry out complete active-space MCSCF (CASSCF) followed by first-order configuration-interaction calculations (FOCI) on 10 electronic states of $ArCl^+$ as a function of internuclear distance. Section II describes the experimental methods and results; Sec. III outlines the theoretical method of calculations, while Sec. IV contains results and discussions.

II. EXPERIMENTAL METHODS AND RESULTS

Collisions of Cl^+ with Ar were measured using a tandem mass spectrometer which has been described previously.[21] It consists of an ion source, an electrostatic analyzer, and a quadrupole mass filter as an input section. The Cl^+ ions were prepared by electron bombardment of CH_3Cl. The beam composition was 40% $Cl^+(^1D_2)$ and 60% $Cl^+(^3P_{0,1,2})$, as determined by an attenuation method.[22] The beam width was 0.1 eV full width at half maximum.

The beam of a Cl^+ ion so prepared then passed through a shallow reaction chamber containing the target

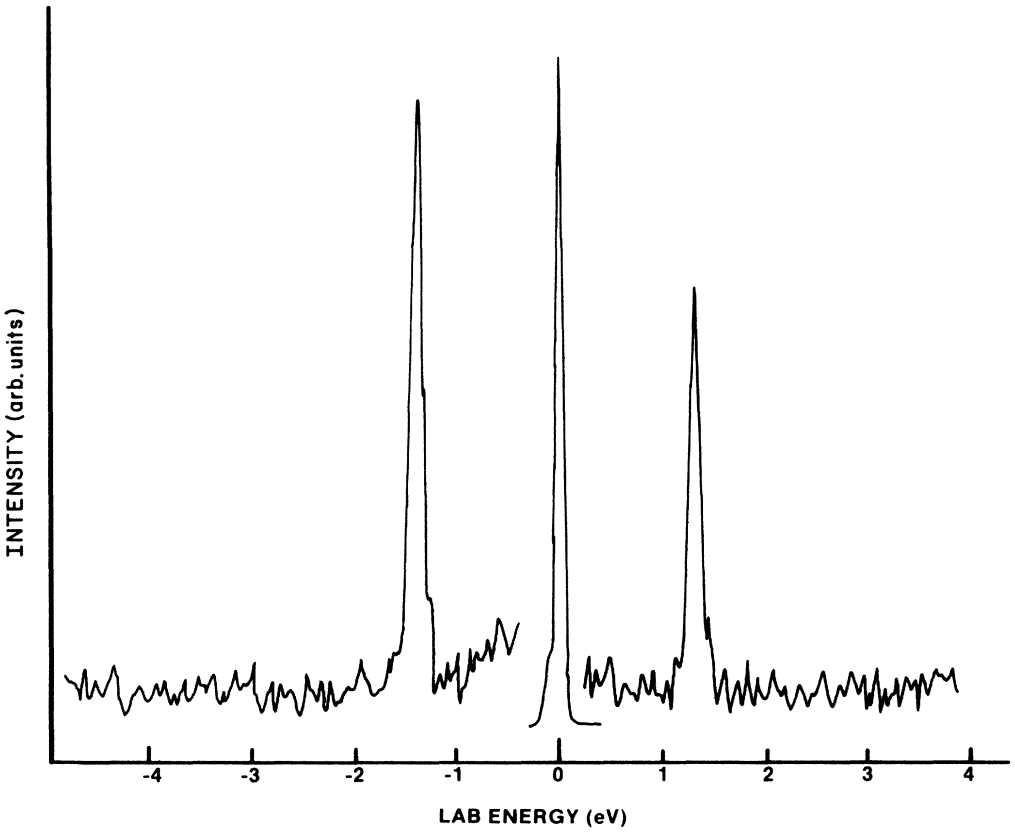

FIG. 1. Kinetic energy spectra of Cl^+ resulting from collisions of Cl^+ with Ar at 10 eV center of mass energy.

gas Ar. The ions scattered 0° to the primary ion-beam direction were then mass analyzed by a second quadrupole mass filter, energy analyzed by an electrostatic analyzer, and detected with an electron multiplier.

The energy spectrum obtained (Fig. 1) consisted of three peaks. The central peak is the unperturbed peak of Cl^+. The Q values of the left and right peaks are -1.42 and 1.38 eV, respectively. The spacing between the $^3P_2$ ground state of Cl^+ and the excited state $^1D_2$ is 1.444 eV. The range of possible Q values is between 1.32 and 1.44 eV depending on whether the lower Cl^+ term involved is $^3P_0$, $^3P_1$, or $^3P_2$. The spacings of the spin-orbit energy levels are too small to be resolved by our instrument. We therefore interpret the "superelastic" peak on the right as corresponding to the transition $Cl^+(^1D_2)\rightarrow Cl^+(^3P_{0,1,2})$ and the "subelastic" peak on the left to the transition $Cl^+(^3P_{0,1,2})\rightarrow Cl^+(^1D_2)$.

III. METHODS OF CALCULATIONS

Table I shows the atomic states of Ar and Cl^+ and Cl and Ar^+ and the molecular states arising from them in the absence of spin-orbit interaction. As one can see, there are many electronic states for $ArCl^+$. Our objec-

TABLE I. Dissociation limits for $ArCl^+$. (Brackets indicate estimated value, see Ref. 28.)

Molecular	Atomic states	Energy (cm^{-1}) Calculated[a]	Experimental[b]
	$Ar + Cl^+$		
$^3\Pi, ^3\Sigma^-$	$^1S + ^3P$	0.0	0.0
$^1\Delta, ^1\Pi, ^1\Sigma^+$	$^1S + ^1D$	14 697	11 652
	$Ar^+ + Cl$		
$^1\Pi(2), ^1\Sigma^+(2), ^1\Sigma^-$ $^1\Delta, ^3\Pi(2), ^3\Sigma^+(2),$ $^3\Sigma^-, ^3\Delta$	$^2P + ^2P$	21 144	22 140
	$Ar + Cl^+$		
$^1\Sigma^+$	$^1S + ^1S$		[27 900]

[a]Without spin-orbit interaction.
[b]From Ref. 28.

TABLE II. Basis sets employed for Ar and Cl.

	Ar		Cl	
Type	Exponent	Contraction coefficient	Exponent	Contraction coefficient
s	25.99	0.003 397	21.51	0.001 075
s	2.336	0.339 128	2.145	0.312 437
s	0.6503	1.0	0.5119	1.0
s	0.2240	1.0	0.1799	1.0
p	16.49	0.008 059	14.55	0.008 368
p	5.255	0.025 053	4.179	0.020 126
p	0.7689	1.0	0.6291	1.0
p	0.2223	1.0	0.1830	1.0
d	0.85	1.0	0.75	1.0

tive is to calculate all the electronic states of $Ar + Cl^+$ which dissociate into $^1S + {}^3P, {}^1S + {}^1D$ limits and a few electronic states which dissociate into $Ar^+(^2P) + Cl(^2P)$ limit.

We employ relativistic effective core potentials for both Ar and Cl atoms reported by Pacios and Christiansen[23] together with the valence Gaussian basis sets optimized for the ground states of the neutral atoms. We contract the first two *s* and *p* functions of Ar and Cl atoms with the *contraction coefficients* shown in Table II. The $(4s4p/3s3p)$ basis set obtained in this way was augmented by a set of *d*-type polarization functions with the exponents shown in Table II.

The orbitals for configuration-interaction calculations were generated using the complete active space MCSCF (CASSCF) method. In this method 14 outer electrons arising from Ar $(3s^23p^6)$ and Cl^+ $(3s^23p^4)$ were distributed in all possible ways among the strongest occupied orbitals of the dissociated atoms which correlate into 3*s* and 3*p* orbitals of Ar and Cl. The CASSCF calculations were actually carried out in the C_{2v} group. The molecule was oriented along the *z* axis which was also chosen as the C_2 axis. In this orientation the active space in the CASSCF consisted of four a_1, two b_2, and two b_1 orbitals.

The configuration-interaction (CI) calculations were carried out using the first-order CI (FOCI) method. The FOCI calculations included all configurations in the CASSCF plus the configurations generated by distributing 13 electrons in the internal space and one electron in the external space in all possible ways. Table III gives the configuration counts in the C_{2v} group for various spatial and spin symmetries.

Relativistic configuration-interaction (RCI) calculations including spin-orbit interaction are carried out for the low-lying states of $ArCl^+$ with the objective of estimating the spin-orbit corrections. These calculations are carried out for the $^3\Pi_2$, $^3\Pi_1$, $^3\Pi_{0^-}$, $^3\Pi_{0^+}$, $^3\Sigma_1^-$, $^3\Sigma_{0^+}^-$ states. The two-state calculations included two reference configurations arising from $^3\Pi_2$. The one-state calculations include five reference configurations $(^3\Pi_1, {}^1\Pi_1, {}^3\Sigma_1^-)$. The 0^+ state included six reference configurations arising from $^3\Pi_{0^+}$ and $^3\Sigma_{0^+}^-$. The 0^- state include four reference configurations arising from $^3\Pi_{0^-}$. Single and double excitations were allowed from these reference configurations. CI calculations with the same set of configurations were carried out for the $^3\Pi$ and $^3\Sigma^-$ states without the spin-orbit term. The difference between the two results is taken to be the spin-orbit correction. The RCI calculations were carried out primarily to estimate spin-orbit effects.[24] These calculations were made following a SCF calculation of the $^3\Pi$ state which employed a double-ζ plus polarization Slater-type orbital (STO) basis set. The MCSCF-FOCI calculations were carried out using

TABLE III. Dimensions of the CASSCF and FOCI spaces. Configuration counts are for the C_{2v} symmetry group.

State	CASSCF	FOCI
$^1A_1$	16	1312
$^3A_2$	4	1476
$^3B_1$	8	1576
$^1B_1$	8	1184

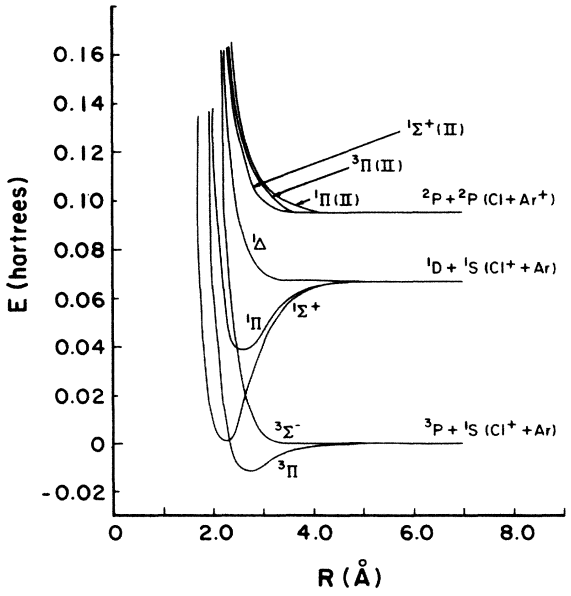

FIG. 2. Potential-energy curves of low-lying states of $ArCl^+$.

TABLE IV. Spectroscopic properties of low-lying states of $ArCl^+$.

State	R_e (Å)	T_e (cm^{-1})	ω_e (cm^{-1})	D_e (eV)
$^3\Pi$	2.71	0.0	191	0.32
$^1\Sigma^+$	2.16	2353	421	1.85
$^1\Pi$	2.60	10911	286	0.79

Balasubramanian's modified version of the GAMESS package of codes[25] to include relativistic effective core potentials, while the RCI calculations were carried out using one of the author's (K.B.) modified version of the code developed earlier based on the method described in Ref. 26.

IV. RESULTS AND DISCUSSION

Table IV shows the spectroscopic properties of the three bound states of $ArCl^+$ obtained using the CASSCF-FOCI methodology. The ground state of $ArCl^+$ is found to be a bound $^3\Pi$ state with a somewhat smaller vibrational frequency of 342 cm^{-1} compared to the somewhat more bound $^1\Pi$ and $^1\Sigma^+$ states which dissociate into $Ar(^1S)+Cl^+(^1D)$ atoms.

Figure 2 shows the potential-energy surfaces of all the electronic states dissociating into $Ar(^1S)+Cl^+(^3P)$, $Ar(^1S)+Cl^+(^1D)$ and some of the electronic states dissociating into $Ar^+(^2P)+Cl(^2P)$ states. Among the electronic states dissociating into the ground-state $Ar(^1S)+Cl^+(^3P)$ atoms, the $^3\Pi$ state is bound while the $^3\Sigma^-$ state is repulsive. The $^1\Sigma^+$ state dissociating into $Ar(^1S)+Cl^+(^1D)$ is the most strongly bound state. The $^1\Pi$ state which dissociates into these atoms is also bound but somewhat less in comparison to the $^1\Sigma^+$ state. All the states calculated here which dissociate into $Ar^+(^2P)+Cl(^2P)$ are repulsive.

As one can see from Fig. 2, the strongly bound $^1\Sigma^+$ curve is crossed by both $^3\Pi$ and $^3\Sigma^-$ curves dissociating into $Ar(^1S)+Cl^+(^3P)$. Table V shows the various curve crossing distances and the energies at the crossings. In the Landau-Zener model the energy transfers in the collision of two species take place at the points of intersections of the potential-energy surfaces of the intermediate complex. As one can see from Table V and Fig. 2, the $^3\Pi$ curve crosses with the $^1\Sigma^+$ bound curve at 2.35 Å which is about 0.19 Å larger than the R_e of the $^1\Sigma^+$ state. The crossing of the repulsive $^3\Sigma^-$ state occurs at a much larger distance (0.44 Å larger than the R_e of the $^1\Sigma^+$ state). This feature of the potential-energy surfaces of $ArCl^+$ is reminiscent of the surfaces of NeF^+. Hotokka *et al.*[14] have shown that the $^3\Pi$ curve crosses at about 0.07 Å larger than the R_e of the $^1\Sigma^+$ while the $^3\Sigma^-$ curve crosses approximately 0.24 Å larger than the R_e of the $^1\Sigma^+$ state. Since for $ArCl^+$ the $^1\Sigma^+$ state is more bound in comparison to NeF^+ (~0.22 eV more bound) crossing at 0.19 Å larger than R_e in comparison to NeF^+ for which the crossing occurs at 0.07 Å larger than its R_e, the predissociation in $ArCl^+$ would occur at a higher vibrational level. The lifetime is determined by the crossings of the various curves. Although the $^3\Pi$ curve crosses at a shorter distance than $^3\Sigma^-$, since $^3\Pi$ is bound, the molecule would be long lived in this state. The lifetime of $ArCl^+$ is this primarily determined by the $^1\Sigma^+$-$^3\Sigma^-$ crossing, which occurs at a considerably larger distance.

TABLE V. Curve crossings for $ArCl^+$. The energies of the crossings are with respect to $Ar(^1S)+Cl^+(^3P)$.

State-state	R (Å)	E (cm^{-1})
$^3\Pi$-$^1\Sigma^+$	2.35	1750
$^3\Sigma^-$-$^1\Sigma^+$	2.60	4390
$^1\Pi$-$^3\Sigma^-$	2.46	8560

The classical turning points of a vibrational level determine the classically allowed or forbidden region for predissociation. If the crossing occurs above the classical turning points of a vibrational level of the species, then the species can have long lifetimes in this level. As the crossing occurs above many vibrational levels, the lifetime is higher. Thus the lifetime of $ArCl^+$ is certainly larger than NeF^+ since the crossing occurs above the classical turning points of at least the first two vibrational levels. The actual lifetimes are very sensitive to the exact crossings which we believe cannot be located so accurately as to determine the lifetimes exactly at the present level of theory which is adequate for many other purposes.

The crossing of the $^3\Sigma^-$ state at a larger distance than $^3\Pi$ would imply that this crossing occurs above more vibrational levels than the corresponding crossing of $^3\Pi$.

The accuracies of the calculations described here can be estimated by comparing the calculated and experimental asymptotic limits. Table I shows the calculated and experimental splittings of the atomic states. As one can see from Table I, the calculated separation of the $Ar^+(^2P)+Cl(^2P)$ level with respect to the $Ar(^1S)+Cl^+(^3P)$ level is quite accurate in comparison to the experimental results. The calculated asymptotic limit of the $Ar(^1S)+Cl^+(^1D)$ atoms, however, is somewhat higher than the experimental value of 11 652 cm^{-1}. This difference is attributed to correlation, basis-set errors, and the omission of the spin-orbit term in Table I. Although the CASSCF-FOCI approach gives quite accurate results for the lowest states, the excited-state energies could be about 10–15% higher than the true values. The higher asymptotic limit is consistent with the calculations of Hotokka *et al.*[14] who also found that the $Ne(^1S)+F^+(^1D)$ limit is somewhat higher than the experimental value while the relative error made in calculating the $Ne^+(^2P)+F(^2P)$ limit is smaller. Thus the crossings of the potential-energy curves would be shifted to larger values if one corrects for the asymptotic difference in energies.

The theoretical CASSCF-FOCI D_e value for the $^1\Sigma^+$

TABLE VI. Mulliken population analysis and dipole moments for low-lying states of $ArCl^+$.

State	R (Å)	Gross Ar total	Gross Cl total	Ar s	Ar p	Ar d	Cl s	Cl p	Cl d	Overlap	Dipole moment (Debye)
$^3\Pi$	2.75	7.814	6.186	1.986	5.813	0.015	1.958	4.181	0.046	0.042	4.4105
$^3\Sigma^-$	2.75	7.959	6.041	1.990	5.960	0.009	1.951	4.037	0.053	0.0908	6.2224
$^1\Sigma^+$	2.25	7.497	6.503	1.964	5.492	0.041	1.959	4.499	0.045	0.1616	0.203
$^1\Pi$	2.50	7.590	6.410	1.979	5.586	0.024	1.963	4.404	0.043	0.0226	1.460

state of $ArCl^+$ is 1.85 eV. The CASSCF-FOCI calculations on comparable main group diatomics[15–18] have yielded D_e's within 10–20% of the experimental results. The CASSCF-FOCI results are consistently lower than the experimental results due to missing higher-order correlation corrections which tend to lower the molecular state in comparison to the atomic states. Thus we believe that the calculated D_e of 1.85 eV is a lower bound. An experimental value of 1.75 eV has been inferred by Sharma and Koski[27] through collision-induced dissociation of $ArCl^+$ in Ar. These two results are in excellent agreement suggesting that the D_e of $ArCl^+$ should be between 1.75–2.0 eV.

Table VI shows the Mulliken population analysis of the $^3\Pi$, $^1\Sigma^+$, $^1\Pi$, and $^3\Sigma^-$ states of $ArCl^+$ and the dipole moments. For the $^3\Pi$, $^1\Sigma^+$, and $^1\Pi$ states, the analysis is near the equilibrium geometries of the states while for the $^3\Sigma^-$ repulsive state we report the result at 2.75 Å (near r_e of $^3\Pi$). The total gross population of the $^3\Pi$ state at its equilibrium geometry reveals that the Ar atom is nearly neutral and Cl carries the positive charge. For the $^1\Sigma^+$ and $^1\Pi$ states, however, there is considerable charge transfer from Ar to Cl^+. For the $^1\Sigma^+$ state,in fact, the positive charge is equally shared between Ar and Cl atoms. This is consistent with the calculated dipole moments in Table VI. The dipole moment of the $^1\Sigma^+$ state is very small (0.2 D), while the $^3\Pi$ state has a large dipole moment (4.4 D) at its equilibrium geometry. The $^1\Pi$ state which dissociates to the same asymptotic limit as $^1\Sigma^+$ has a larger dipole moment (1.46 D) than $^1\Sigma^+$.

Next, we calculate the spin-orbit effects for $ArCl^+$ through the relativistic configuration-interaction method. First, we discuss the atomic splittings. Table VII shows the asymptotic spin-orbit splittings of the low-lying states of $ArCl^+$ in ω-ω to j-j coupling. The atomic splittings shown in that table were taken from Ref. 28. Note that the spin-orbit splittings of the states which correlate into the $Ar + Cl^+$ limit are primarily determined by the spin-orbit splittings of Cl^+, while the spin-orbit splitting of states which dissociate into $Ar^+ + Cl$ limit would depend on the splitting of Ar^+ and Cl. Further, the closed-shell molecular states would have near-zero spin-orbit splitting even if the spin-orbit splitting is substantial at the dissociation limit. For example, the $^1\Sigma_g^+$ ground state of Br_2 is almost zero (67 cm^{-1}) (Ref. 24), while the atomic $^2P_{3/2}$-$^2P_{1/2}$ splitting of the bromine atom is 3685 cm^{-1}. Thus the spin-orbit splitting of the $^1\Sigma^+$ state of $ArCl^+$ would be close to zero.

The $^3\Pi$ state of $ArCl^+$ would be split into $^3\Pi_{2,1,0^-,0^+}$ components. The $^3\Pi_2$ would be the lowest since this is an inverted $^3\Pi$. The splitting between $^3\Pi_2$-$^3\Pi_1$ states would be equal to the Cl^+ $^3P_2$-$^3P_1$ splitting at very long distance since the spin-orbit splitting of the closed shell $Ar(^1S)$ is zero. The splitting between $^3\Pi_2$ and $^3\Pi_{0^+}$ state would similarly be close to the $^3P_2$-$^3P_0$ of the Cl^+ ion at long distance. The splitting between $^3\Pi_{0^+}$ and $^3\Pi_{0^-}$ is expected to be small at near-equilibrium geometries.

Table VIII shows the magnitude of the spin-orbit effects for the $^3\Pi$ and $^3\Sigma^-$ states of $ArCl^+$ obtained using relativistic CI calculations. The spin-orbit splittings are seen to be somewhat small for $ArCl^+$. The maximum

TABLE VII. Correlation of molecular and atomic states including spin-orbit interaction.

Molecular states	Atomic states	Energy (cm^{-1})[a]
	$Ar + Cl^+$	
$2,1,0^+$	$^1S_0 + ^3P_2$	0.0
$1(II),0^-$	$^1S_0 + ^3P_1$	667
$0^+(II)$	$^1S_0 + ^3P_0$	996
$2(II),1(III),0^+(III)$	$^1S_0 + ^1D_2$	11 652

[a]From Ref. 28.

TABLE VIII. Spin-orbit effects for low-lying states of $ArCl^+$. For the $^3\Pi$ states the values are with respect to $^3\Pi$ without spin orbit. For the $^3\Sigma^-_{0^+,1}$ states, the corrections in energies are with respect to $^3\Sigma^-$ without a spin-orbit term.

	ΔR_e (Å)[a]	$\Delta\omega_e$ (cm^{-1})	ΔE (cm^{-1})
$^3\Pi_2$	0.0	0	−387
$^3\Pi_1$	+0.009	−5	−84
$^3\Pi_{0^+}$	+0.024	−11	+286
$^3\Pi_{0^-}$	0.0	0	+390
$^3\Sigma_1^-$	2.50		0
$^3\Sigma_{0^+}^-$	2.50		+42
$^3\Sigma_1^-$	3.00		0
$^3\Sigma_{0^+}^-$	3.00		+165
$^3\Sigma_1^-$	3.50		0
$^3\Sigma_{0^+}^-$	3.50		424

[a]For $^3\Sigma^-$, the reported values are actual bond lengths since this state has no minimum.

splitting at the equilibrium geometry corresponds to the $^3\Pi_2$-$^3\Pi_{0^-}$ splitting which is 777 cm^{-1}. The shifts in bond lengths are negligible with the exception of the $^3\Pi_{0^+}$ for which the bond length increases by 0.024 Å. The spin-orbit splittings generally increase and reach the maximum value of the atomic Cl^+ splitting reported in Table VII. The spin-orbit contribution to the $^1\Sigma^+$ state would almost be zero. Sine the bond lengths of $^3\Pi_2$, $^3\Pi_1$, and $^3\Pi_{0^-}$ are not affected much by spin-orbit interaction, the crossings of the components with $^1\Sigma^+$ will not be shifted much due to the spin-orbit term.

Next, we compare the Ar-Cl^+ collision with Ne-F^+ and Kr-Br^+ collisions. The potential-energy surfaces of the $ArCl^+$ ion resemble those of NeF^+ calculated earlier by Hotokka *et al.*;[14] however, there are many differences. First, the $^3\Pi$ ground state for $ArCl^+$ is bound in comparison to a repulsive $^3\Pi$ curve for NeF^+. This could be in part because we carry out CI calculations following CASSCF while Hotokka *et al.*[14] carry out CASSCF only but employ a slightly larger active space by including one more π orbital. The $^1\Sigma^+$ state of $ArCl^+$ appears to be more strongly bound than that of NeF^+. As noted before, the crossing of the $^3\Pi$ and $^3\Sigma^-$ surfaces with the bound $^1\Sigma^+$ surface occurs at a somewhat larger distance for $ArCl^+$ in comparison to NeF^+. This combined with the fact that the $^1\Sigma^+$ and $^3\Pi$ states of $ArCl^+$ have deeper wells would imply that the lifetime of $ArCl^+$ should be larger than that of NeF^+.

While there is some resemblance between the potential-energy surfaces of $ArCl^+$ and $KrBr^+$ pairs in the absence of spin-orbit interaction, the spin-orbit effects are much larger for $KrBr^+$. Further, there are many avoided crossings when the spin-orbit term is introduced which change the shapes of the potential-energy surfaces substantially for $KrBr^+$. The $^1\Sigma^+(0^+)$ state of $KrBr^+$ is not as strongly bound as the corresponding state of $ArCl^+$ or NeF^+. The spin-orbit interaction also reduces the D_e in $KrBr^+$. The experimental D_e of the $KrBr^+$ ion is about 1.5 eV. The main difference between the heavier species such as $KrBr^+$ and the lighter species is the dramatically larger spin-orbit effects in heavier species which influence the shapes of the potential-energy surfaces and curve crossings.

V. CONCLUSION

In this investigation the energy transfers in Ar-Cl^+ collisions were studied through a Landau-Zener model. The potential-energy surfaces of all the electronic states which dissociate into $Ar(^1S)+Cl^+(^3P)$, $Ar(^1S)+Cl^+(^1D)$ and some of the electronic states which dissociate into $Ar^+(^2P)+Cl(^2P)$ asymptotes were obtained using a CASSCF-FOCI scheme. These calculations reveal the existence of three bound electronic states ($^3\Pi$, $^1\Sigma^+$, $^1\Pi$). The D_e value of the $^1\Sigma^+$ state which dissociates into $Ar(^1S)+Cl^+(^1D)$ is calculated to be 1.81 eV at the CASSCF-FOCI level of theory. The $^3\Sigma^-$ and $^3\Pi$ curves cross the $^1\Sigma^+$ bound curve at distances larger than R_e of $^1\Sigma^+$. The crossing of $^3\Sigma^-$ with $^1\Sigma^+$ curve occurs at a larger distance than the corresponding crossing of $^3\Pi$ with $^1\Sigma^+$. It is predicted that $ArCl^+$ should be long lived. The Mulliken populational analysis reveals that the positive charge is more localized on Cl for $^3\Pi$ and $^3\Sigma^-$ states while it is equally shared between Ar and Cl atoms for the $^1\Sigma^+$ state and somewhat less for the $^1\Pi$ state. The calculated dipole moment of the $^1\Sigma^+$ state is considerably smaller than that for the $^3\Pi$ state.

ACKNOWLEDGMENTS

K. B. would like to thank the National Science Foundation for support of this work through Grant No. CHE8520556 and the Alfred P. Sloan Foundation and Camille and Henry Dreyfus Foundation for financial support. Some of the computations described here were carried out on the San Diego Cray XMP supercomputer system.

[1]L. G. Piper, J. E. Velazco, and D. W. Setser, J. Chem. Phys. **59**, 3323 (1973).
[2]J. E. Velazco, J. H. Kohs, and D. W. Setser, J. Chem. Phys. **65**, 3468 (1976).
[3]D. L. King, L. G. Piper, and D. W. Setser, J. Chem. Soc. Faraday Trans. III **73**, 177 (1977).
[4]M. Rokini, J. H. Jacobs, and J. A. Mangano, Phys. Rev. A **16**, 2216 (1977).
[5]R. E.Olson and B. Liu, Phys. Rev. A **17**, 1568 (1978).
[6]T. H. Dunning and P. J. Hay, J. Chem. Phys. **66**, 3767 (1977).
[7]J. S. Cohen, W. R. Wadt, and P. J. Hay, J. Chem. Phys. **71**, 2955 (1979).
[8]J. H. Holloway, *Noble Gas Chemistry* (Methuen, London, 1968).
[9]A. Henglein and G. A. Muccini, Angew. Chem. **72**, 630 (1960).
[10]I. Kuen and F. Howorka, J. Chem. Phys. **70**, 595 (1979).
[11]J. Berkowitz and W. A. Chupka, Chem. Phys. Lett. **7**, 447 (1970).
[12]J. Berkowitz, W. A. Chupka, R. L. Guyon, J. H. Holloway, and R. Sphor, J. Phys. Chem. **75**, 1461 (1971).
[13]K. Balasubramanian, J. J. Kaufman, P. C. Hariharan, and W. S. Koski, Chem. Phys. Lett. **129**, 165 (1986).
[14]M. Hotokka, B. Roos, J. B. Delos, R. Srivastava, R. B. Sharma, and W. S. Koski, Phys. Rev. A **35**, 4515 (1987).
[15]K. Balasubramanian, J. Phys. Chem. **90**, 6786 (1986).
[16]K. Balasubramanian, J. Mol. Spectrosc. **123**, 228 (1987).
[17]K. Balasubramanian, J. Mol. Spectrosc. **121**, 465 (1987).
[18]K. Balasubramanian, J. Chem. Phys. **86**, 3410 (1987).
[19]K. Balasubramanian and K. S. Pitzer, Adv. Chem. Phys. **67**, 287 (1987).
[20]K. Balasubramanian and K. S. Pitzer, Int. J. Quantum Chem. **23**, 31 (1984).
[21]K. Wendell, C. A. Jones, J. J. Kaufman, and W. S. Koski, J. Chem. Phys. **63**, 750 (1975).
[22]K. C. Lin, R. S. Cotter, and W. S. Koski, J. Chem. Phys. **61**, 905 (1974).

[23]L. F. Pacios and P. A. Christiansen, J. Chem. Phys. **82**, 2664 (1985).

[24]K. Balasubramanian, Chem. Phys. (to be published).

[25]The original GAMESS package was assembled by M. Dupuis, D. Spangler, and J. Wendoloski. The modified version (1.03), which is an upgrade to include relativistic effective potentials, was prepared by K. Balasubramanian.

[26]P. A. Christiansen, K. Balasubramanian, and K. S. Pitzer, J. Chem. Phys. **76**, 5087 (1982).

[27]R. B. Sharma and W. S. Koski (unpublished).

[28]C. E. Moore, *Table of Atomic Energy Levels,* Natl. Bur. Stand. (U.S.) Circ No. 467 (U.S. GPO, Washington, D.C., 1971), Vol. 1.